

Predictive Modeling of Mass Flow Rates of Lunar Regolith Simulants. J. M. Long-Fox^{1,2}, P. B. Easter^{1,3}, Z. A. Landsman^{1,4}, and D. T. Britt^{1,5} ¹University of Central Florida, 4111 Libra Drive Suite 430, Orlando, FL 32816, USA ²jared.long-fox@ucf.edu, ³peaster@knights.ucf.edu, ⁴zoe.landsman@ucf.edu, ⁵dbritt@ucf.edu

Introduction: Lunar construction and *in situ* resource utilization (ISRU) processes will likely involve the transport of regolith using conveyor and funnel systems. To maximize the efficiency of such systems, systematic characterization of the granular flow properties of lunar regolith is necessary, especially since the highly angular grains of lunar regolith [1] are expected to decrease flow rates and cause cohesive arches to form in funnels. Estimates of the amount of regolith that can flow through a funnel of a given outlet diameter are key for developing efficient lunar systems. As such, this study applies the theory of mass flow rates of granular materials presented in Beverloo et al. [2] to develop predictive equations for the mass flow rates of the Exolith Lab lunar highlands simulant (LHS-1) [3] and lunar mare simulant (LMS-1) [4] out of funnels of various outlet diameters.

Methods: Mass flow rate data used here, from [5], was collected by flowing 5 independent samples of 500 ± 5 g of LHS-1 and LMS-1 through polycarbonate funnels (being vibrated by four 3V coin-style vibration motors) with varying outlet diameters (2.5 cm, 3.0 cm, 3.5 cm, 4.0 cm, 4.5 cm, and 5.0 cm, all ± 0.1 cm) into a container resting on a laboratory balance that is capable of serial communications. As the simulant flowed out of the funnels, the scale sends mass data to a laptop running a Python script that logs cumulative mass and time elapsed to an ASCII text file at a rate of ~ 10 Hz. The cumulative mass and time elapsed data are used to determine a linear flow rate (g/s) as the ratio of final mass to elapsed time at which the mass on the balance is constant (the end of flow).

The measured mass flow rates of LHS-1 and LMS-1 were analyzed using the relationship proposed by [2]:

$$W = C\rho_b\sqrt{g}(D_0 - Kd_p)^{5/2} \quad (1)$$

Where W is mass flow rate (g/s), ρ_b is bulk density, g is the acceleration of gravity (cm^2/s), d_p is particle diameter (cm), D_0 is outlet diameter (cm), and C is an empirical discharge parameter, and K is an empirical shape parameter. All values except C and K are known, so these are optimized in an adaptive Monte Carlo analysis. This optimization method uses the mass flow rate data as the calibration targets to minimize the residual sum of squared errors (SSE) of model predictions to data. Since it is not possible to solve for both C and K simultaneously, a random value of the nonlinear K is taken from

a normal distribution and substituted into Equation 1, leaving C as the only unknown value, which is calculated using a least squares linear inversion. The randomly sampled K and C are then substituted into Equation 1 to create a forward model (prediction) of mass flow rates, and the results of each forward model are compared to measured flow rates and error relative to the data is calculated. This random sampling of K , inversion for the corresponding C , and forward model error analysis is repeated 10,000 times for 10 adaptations. After each adaptation of 10,000 random samples of K and corresponding C , the search distribution is adjusted to have its mean be the best fit value of K found so far (initial value of 1.4 [2]) and the standard deviation (width of search, initially 100) is shrunk according to:

$$S_i = S_0 e^{-a/2} \quad (2)$$

Where S_i is the adaptation standard deviation, S_0 is the initial standard deviation and a is the current adaptation ($a = 0-9$, a total of 10 adaptations), and S_i reaches a final 1σ precision of 1.11 on the tenth adaptation ($a = 9$). Outputs of the adaptive Monte Carlo analysis of mass flow rates based on [2] include best fit parameter estimates and 2σ (95%) confidence intervals.

Results: The adaptive Monte Carlo analysis results for LHS-1 and LMS-1 are given in Table 1. Figure 1 shows the best fit mass flow rate predictions using best fit LHS-1 parameter values (A), as well as the 2σ confidence intervals for K (B) and C (C). Figure 2 shows the best fit mass flow rate predictions using best fit LMS-1 parameter values (A), as well as the 2σ confidence intervals for K (B) and C (C).

Table 1. Beverloo et al. [2] parameter estimates for LHS-1 and LMS-1 with 2σ uncertainties.

	LHS-1	LMS-1
K	$-34.63 \pm \begin{smallmatrix} 37.88 \\ 40.88 \end{smallmatrix}$	$-214.91 \pm \begin{smallmatrix} 44.62 \\ 47.85 \end{smallmatrix}$
C	$0.051 \pm \begin{smallmatrix} 0.007 \\ 0.006 \end{smallmatrix}$	$0.062 \pm \begin{smallmatrix} 0.007 \\ 0.006 \end{smallmatrix}$

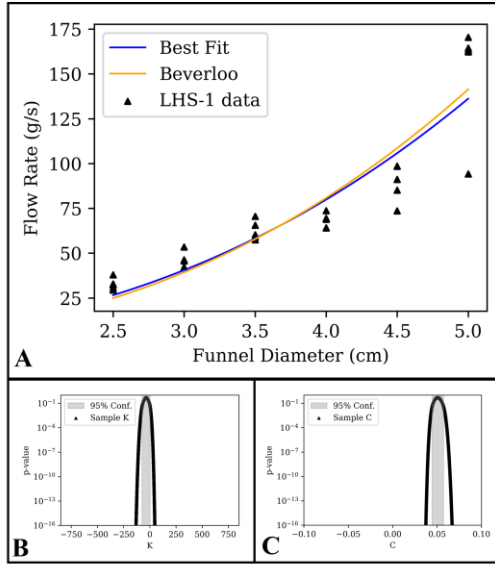


Figure 1. (A) Mass flow rate predictions and measurements for LHS-1. (B) Randomly sampled LHS-1 K values, p-values, and 95% confidence interval. (C) Randomly sampled LHS-1 C values, p-values, and 95% confidence interval.

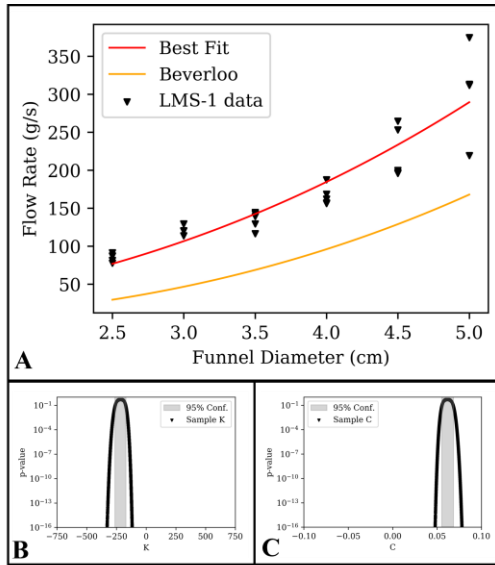


Figure 2. (A) Mass flow rate predictions and measurements for LMS-1. (B) Randomly sampled LMS-1 K values, p-values, and 95% confidence interval. (C) Randomly sampled LMS-1 C values, p-values, and 95% confidence interval.

Discussion: The best fit value of shape parameter K [1] for LHS-1 is significantly lower in magnitude than that of LMS-1, indicating that particle geometry (shape and size) affects flow characteristics. The average particle size for LHS-1 is 90 μm but ranges from less than

0.04 μm to 1000 μm [3] and the average particle size for LMS-1 is 90 μm but ranges from less than 0.04 μm to 1000 μm [4], so this difference may contribute to differences in the shape parameter. LHS-1 and LMS-1 are created using identical percussive crushing methods, but the differences in mineralogy results in different particle morphology when crushed, which may explain the differences observed in K . The 2σ confidence intervals on C overlap for LHS-1 and LMS-1, but the best fit value for LHS-1 is lower than that of LMS-1. The similarity in C , the discharge coefficient [2], indicates that the density and gravity contributions to flow are similar for these simulants, despite LHS-1 having lower bulk density than less dense than LMS-1 (1.39 g/cm^3 [6] and 1.65 g/cm^3 [4], respectively). The differences in K and similarity of C indicate that bulk density is a less significant factor in determining flow rates of mineralogically-accurate lunar regolith highlands and mare regolith simulants, whereas particle shape and size are dominant controlling factors.

The estimated values of K and C for LHS-1 and LMS-1 are very different from the standard values for K (1.4) and C (35) given in [2], and these suggested all-purpose values give results that underpredict mass flow rates for LMS-1 (Figure 2B) but give a suitable fit for LHS-1 (Figure 1A). Differences in best fit values found in this study compared to those recommended by [2] are attributed to the relatively wide particle size distributions and small particle size of LHS-1 and LMS-1, as Equation 1 was developed for a seeds and other particles of uniform size larger than 0.5 mm [1, 7]. Building on the work of [2], Mankoc et al. [7] develop equations for mass flow rate that can accommodate particle diameters less than 0.5 mm, which are also being investigated to better inform on system requirements for lunar regolith transport and storage.

Conclusion: Special consideration must be given to designing regolith transport and processing systems, as the non-uniform particle size distribution, irregular shape, and mineralogic composition of lunar regolith and its simulants directly alter the characteristics of the granular flow, as shown here by mineralogically-accurate lunar highlands (LHS-1) and mare (LMS-1) simulants.

References: [1] Carrier et al. (1991), *The Lunar Sourcebook: a user's guide to the moon*, Chapter 9. [2] Beverloo et al. (1961), *Chem. Eng. Sci.* 15, 260-269. [3] Exolith Lab (2021), *LHS-1 Fact Sheet*, February 2022. [4] Exolith Lab (2021), *LMS-1 Fact Sheet*, February 2022. [5] Long-Fox et al. (2021), *NASA Lunar Surface Science Workshop*, August 18-19, 2021. [6] Long-Fox et al. (2022), *ASCE Earth and Space Conference 2022*, in review. [7] Mankoc et al. (2007), *Granular Matter* 9, 407-414.